Green's function method for the radiative transfer problem. I. Homogeneous non-Lambertian surface

Alexei Lyapustin and Yuri Knyazikhin

An application of the Green's function method to the one-dimensional radiative transfer problem with a non-Lambertian surface is described. This method separates atmospheric radiative transport from the lower boundary condition and allows expressing a solution analytically for an arbitrary surface reflectance. In the physical sense, the Green's function represents bidirectional atmospheric transmission for the unitary radiance source located at the bottom of the atmosphere. The boundary-value problem for the Green's function is adjoint to the problem for atmospheric path radiance, and therefore it can be solved by use of existing numerical methods by reversal of the direction of light propagation. From an analysis of an exact operator solution and extensive numerical study, we found two accelerating parameterizations for computing the surface-reflected radiance. The first one is a maximum-eigenvalue method that is comparable in accuracy with rigorous radiative transfer codes in calculations with realistic land-cover types. It requires a total of the first three orders of the surface-reflected radiance. The second one is based on the Lambertian approximation of multiple reflections. Designed for operational applications, it is much faster: Already the first-order reflected radiance ensures an average accuracy of better than 1%. © 2001 Optical Society of America

OCIS codes: 290.4210, 010.1300, 010.1310, 010.1320.

1. Introduction

The numerical methods of one-dimensional atmospheric radiative transfer, such as adding–doubling,[1] spherical harmonics,[2] or discrete ordinates,[3] have traditionally been developed for the problem with a Lambertian surface. Anisotropic reflectance, if considered, is usually treated by means of numerical integration.[4] The successive orders of scattering code,[5] popular within the remote-sensing community, uses analytical approximations by Tanre *et al.*[6] to account for anisotropic surface properties. Recently we generalized the Marshak boundary condition of the method of spherical harmonics (MSH) for non-Lambertian reflectance[7] and used the rigorous numerical solution in applied research.[8]

In spite of wide opportunities for various applications offered by numerical codes, the lack of analytical solutions restricts data analysis and the development of efficient inversion algorithms. We encountered this inconvenience in practice in the problem of iterative retrieval of the bidirectional reflectance distribution function (BRDF) of a surface from multiangle radiance measurements by use of the MSH.[9] Given the atmospheric conditions, the full radiative transfer problem had to be solved anew in each iteration because the lower boundary condition had changed.

In this paper, we use the Green's function method to derive an analytical solution for the radiance over a surface with arbitrary reflective properties. The concept of the Green's function, developed in neutron transport several decades ago,[10] offers a powerful approach to solving the radiative transfer problem with complex boundary conditions and internal sources. It entails reformulating the general problem in terms of simpler basic subproblems and expressing the general solution as a superposition of these basic solutions. The virtues of the Green's function method in the problem of atmospheric radiative transport were demonstrated earlier.[11,12] Here we offer further development of this method. It is worth mentioning that the Green's function technique is closely related to the adding–doubling method,[1,13] which results in the similarity of the operator equations derived in Section 2 for the Green's function method and the

A. Lyapustin (alyapust@pop900.gsfc.nasa.gov) is with the Joint Center for Earth Systems Technology, University of Maryland Baltimore County, and the NASA Goddard Space Flight Center, Mail Code 920, Greenbelt, Maryland 20771-0000. Y. Knyazikhin is with the Department of Geography, Boston University, Boston, Massachusetts 02215.

Received 2 January 2001; revised manuscript received 22 March 2001.

0003-6935/01/213495-07$15.00/0

corresponding matrix equations of the adding–doubling method.

2. Radiative Transfer Problem and Its Formal Solution

Let us consider a horizontally homogeneous atmosphere bounded by a uniform non-Lambertian surface. Given the atmospheric optical thickness $\tau(z)$, the single-scattering albedo $\omega(z)$, and the scattering function $\chi(z, \gamma)$, the radiance at altitude z in direction s can be found as a solution of the following boundary-value problem:

$$\mu \frac{\partial I(\tau; s)}{\partial \tau} + I(\tau; s) = \frac{\omega\tau}{4\pi} \int_{\Omega} \chi(\tau, \gamma) I(\tau; s') \mathrm{d}s' + \frac{\omega\tau}{4} \chi(\tau, \gamma_0) S_\lambda \exp(-\tau/\mu_0), \quad (1)$$

$$I(0; s) = 0, \ \mu > 0, \quad (1a)$$

$$I(\tau_0; s) = S_\lambda \mu_0 \exp(-\tau_0/\mu_0) \rho(s_0, s) + \frac{1}{\pi} \int_{\Omega^+} I(\tau_0; s') \rho(s', s) \mu' \mathrm{d}s', \quad \mu < 0. \quad (1b)$$

In our notation, $s = (\theta, \phi)$ defines the direction of propagation with the zenith and the azimuthal angles θ and ϕ. The Z axis is pointed downward, so the cosine of the zenith view angle is $\mu > 0$ for downward directions and $\mu \le 0$ otherwise. For convenience in the subsequent presentation, we utilize an operator form of notation[14] with the differential operator $[\hat{L}_1 = \mu(\partial/\partial\tau) + 1]$ and integral operators of scattering

$$\left[\hat{S} = (\omega\tau/4\pi) \int_{\Omega} \mathrm{d}s' \chi(\tau, \gamma) \cdots \right]$$

and of surface reflection

$$\left[\hat{R} = (1/\pi) \int_{\Omega^+} \mathrm{d}s' \rho(s', s) \mu' \ldots \right].$$

The subscripts or superscripts $(+)$ and $(-)$ indicate downward $(\mu > 0)$ and upward $(\mu < 0)$ directions, respectively. For example, the expression $J_-(\tau_0) = \hat{R}J_+(\tau_0)$ is equivalent to $J(\tau_0; s) = (1/\pi) \int_{\Omega^+} J(\tau_0; s') \rho(s', s) \mu' \mathrm{d}s'$ at $\mu < 0$.

Let us apply the Green's function technique to problem (1) to separate the lower boundary condition from calculations of atmospheric functions. First, let us decompose the total signal into the path radiance $D(\tau, s_0, s)$ and surface-reflected radiance $J(\tau; s_0, s)$:

$$I(\tau; s_0, s) = D(\tau; s_0, s) + J(\tau; s_0, s). \quad (2)$$

These radiance components obey the following problems:

$$\hat{L}_1 D = \hat{S} D + S_\lambda \frac{\omega\tau}{4} \chi(\tau, \gamma_0) \exp(-\tau/\mu_0), \quad (3)$$

$$D_+(0) = 0, \ D_-(\tau_0) = 0; \quad (3a)$$

$$\hat{L}_1 J = \hat{S} J, \quad (4)$$

$$J_+(0) = 0, \quad J_-(\tau_0) = \hat{R} I_+^0(\tau_0) + \hat{R} J_+(\tau_0). \quad (4a)$$

In lower boundary condition (4a), $I_+^0(\tau_0)$ denotes the directional surface irradiance created by the directly transmitted sunlight and path radiance:

$$I_+^0(\tau_0) \equiv I^0(\tau_0, s) = \pi S_\lambda \exp(-\tau_0/\mu_0) \delta(s - s_0) + D(\tau_0; s_0, s), \ \mu > 0. \quad (5)$$

The term $\hat{R} I_+^0(\tau_0) = J_-^{(1)}(\tau_0)$ describes the first-order reflection, and the term $\hat{R} J_+(\tau_0)$ describes the nonlinear interactions of multiple bouncing of photons between the surface and the atmosphere.

The solution of problem (4) can be represented as a series in orders of reflection from the surface:

$$J(\tau; s) = \sum_{k \ge 1} J^{(k)}(\tau, s). \quad (6)$$

Redenoting the directional surface irradiance $I_+^0(\tau_0)$ as $J_+^{(0)}(\tau_0)$ for generality, we can write the following recurrent system of subproblems for different orders of reflection $(k \ge 1)$:

$$\hat{L}_1 J^{(k)} = \hat{S} J^{(k)}, \quad (7)$$

$$J_+^{(k)}(0) = 0, \quad J_-^{(k)}(\tau_0) = \hat{R} J_+^{(k-1)}(\tau_0). \quad (7a)$$

By definition,[14] the solution of problem (7) can be analytically expressed by the Green's function $G(\tau; s_1, s)$ of the second kind and boundary values as

$$J^{(k)}(\tau; s) = \int_{\Omega^-} G(\tau; s_1, s) J^{(k)}(\tau_0, s_1) \mathrm{d}s_1. \quad (8)$$

The substitution of Eq. (8) into problem (7) shows that function $G(\tau; s_1, s)$ satisfies the problem, which no longer depends on surface properties:

$$\hat{L}_1 G = \hat{S} G, \quad (9)$$

$$G_+(0) = 0, \quad G_-(\tau_0) = \delta(s - s_1), \ \mu < 0. \quad (9a)$$

Thus the Green's function describes the solely atmospheric radiative transport and serves to find radiance in an arbitrary direction and altitude in the atmosphere, given its angular distribution at the surface level [Eq. (8)].

In numerical calculations, it is inconvenient to have a δ function in the boundary condition. The separation of the diffuse (continuous) component

$G^d(\tau; s_1, s)$ and direct (discontinuous) component in the Green's function,

$$G(\tau; s_1, s) = G^d(\tau; s_1, s),\ \mu > 0, \tag{10a}$$

$$G(\tau; s_1, s) = \exp[-(\tau_0 - \tau)/|\mu_1|]\delta(s - s_1) + G^d(\tau; s_1, s),\ \mu < 0, \tag{10b}$$

leads to the transport problem for the diffuse Green's function:

$$\hat{L}_1 G^d = \hat{S} G^d + \frac{\omega(\tau)}{4\pi} \chi(\tau; \gamma_1)\exp[-(\tau_0 - \tau)/|\mu_1|], \tag{11}$$

$$G_+^d(0) = 0, \quad G_+^d(\tau_0) = 0, \tag{11a}$$

where γ_1 is the angle of scattering from the original direction of propagation s_1 into direction s.

We can see that problem (11) is adjoint to the problem for path radiance (3), provided that the source of irradiation is unitary ($\pi S_\lambda = 1$) and located at the bottom of the atmosphere. Therefore we can calculate the diffuse Green's function by using existing numerical codes for the path radiance by reversing the direction of light propagation or, in other words, by setting the atmospheric layers in reverse order and normalizing the result by πS_λ. When the atmosphere is homogeneous, problem (11) becomes identical to the problem for path radiance at substitution $\tau \to \tau_0 - \tau$ and $s_0 \to s_1$.

Let us now introduce an integral operator $\hat{\Gamma}_{\tau,s}$ corresponding to integral transformation (8):

$$\hat{\Gamma}_{\tau,s} = \int_{\Omega^-} \mathrm{d}s_1 G(\tau; s_1, s) \ldots . \tag{12}$$

According to accepted notation, operators $\hat{\Gamma}_{\tau_0}^+$ and $\hat{\Gamma}_{\tau_0}^-$ describe the bidirectional atmospheric transmittance in backward ($\mu > 0$) and forward ($\mu < 0$) directions, respectively, for the source illuminating the atmosphere from below ($\mu_1 < 0$). Using these operators, we can establish the recurrent relation between successive orders of upwelling radiance at the surface level:

$$J_-^{(k)}(\tau_0) = \hat{R}\hat{\Gamma}_{\tau_0}^+ J_-^{(k-1)}(\tau_0). \tag{13}$$

The total surface-reflected radiance is the sum of all orders of reflection:

$$\begin{aligned} J_-(\tau_0) &= \sum_{k\geq 1} J_-^{(k)}(\tau_0) \\ &= \left[\sum_{k\geq 0} (\hat{R}\hat{\Gamma}_{\tau_0}^+)^k\right]\hat{R}J_+^{(0)}(\tau_0) \\ &= (\hat{I} - \hat{R}\hat{\Gamma}_{\tau_0}^+)^{-1}\hat{R}J_+^{(0)}(\tau_0). \end{aligned} \tag{14}$$

In Eq. (14), $\hat{I}$ is a unitary operator. The formal folding of the geometric progression $\Sigma_{k\geq 0} (\hat{R}\hat{\Gamma}_{\tau_0}^+)^k$ into an inverse operator $(\hat{I} - \hat{R}\hat{\Gamma}_{\tau_0}^+)^{-1}$ is based on the fact that the norm[14] of operator $\hat{R}\Gamma_{\tau_0}{}^+$ is less than one,[15] which physically is a consequence of the energy-conservation law. In an arbitrary direction at atmospheric level $\tau(z)$, the radiance reflected from the surface is given by

$$J(\tau; s) = \hat{\Gamma}_{\tau,s} J_-(\tau_0) = \hat{\Gamma}_{\tau,s}(\hat{I} - \hat{R}\hat{\Gamma}_{\tau_0}^+)^{-1}\hat{R}J_+^{(0)}(\tau_0). \tag{15}$$

The total radiance at the top of the atmosphere can now be written as

$$I(\tau = 0; s_0, s) = D(0; s_0, s) + \hat{\Gamma}_{\tau_0}^-(\hat{I} - \hat{R}\hat{\Gamma}_{\tau_0}^+)^{-1} \times \hat{R}J_+^{(0)}(\tau_0), \quad \mu < 0. \tag{16}$$

Equation (16) generalizes the well-known formula of Chandrasekhar,[16] originally derived for a Lambertian surface in the case of an arbitrary surface reflectance. Here, the multiple reflections of photons between the surface and the atmosphere are taken into account by the inverse operator $(\hat{I} - \hat{R}\hat{\Gamma}_{\tau_0,s}^+)^{-1}$.

Let us now show that Chandrasekhar's expression for the isotropic surface is a particular case of general solution of Eq. (16). For isotropic reflection, the operators are transformed as follows:

(1) We have

$$\hat{R}J_+^{(0)}(\tau_0) = qE_0(\mu_0), \tag{17a}$$

where

$$E_0(\mu_0) = S_\lambda \mu_0 \exp(-\tau_0/\mu_0) + (1/\pi)\int_{\Omega^+} D(\tau_0; s_0, s)\mu \mathrm{d}s$$

is the surface irradiance that is due to the direct sunlight and path radiance.

(2) Because the angular distribution of the reflected radiance $J_-^{(k)}(\tau_0)$ is isotropic,

$$\hat{R}\hat{\Gamma}_{\tau_0}^+ J_-^{(k)}(\tau_0) = qJ_-^{(k)}(\tau_0)\,\frac{1}{\pi}\int_{\Omega^+} \mu'\mathrm{d}s' \times \int_{\Omega^-} G^d(\tau_0; s_1, s')\mathrm{d}s_1 = qc_0 J_-^{(k)}(\tau_0), \tag{17b}$$

where

$$c_0 = (1/\pi)\int_{\Omega^+} \mu'\mathrm{d}s' \int_{\Omega^-} G^d(\tau_0; s_1, s')\mathrm{d}s_1$$

is a spherical albedo of atmosphere. Furthermore, the total surface-reflected radiance becomes

$$J_-(\tau_0) = \sum_{k\geq 1} J_-^{(k)}(\tau_0) = \left[\sum_{k\geq 1} (qc_0)^{k-1}\right]\hat{R}J_+^{(0)}(\tau_0) = \frac{qE_0(\mu_0)}{1 - qc_0}. \quad (17c)$$

(3) Finally, because of the isotropic angular distribution of the surface-reflected radiance, operator $\hat{\Gamma}_{\tau_0}^{-}$ becomes a scalar function:

$$\hat{\Gamma}_{\tau_0}^{-} = \int_{\Omega^-} G(0; s_1, s)\mathrm{d}s_1 = \exp(-\tau_0/|\mu|) + \int_{\Omega^-} G^d(0; s_1, s)\mathrm{d}s_1 = T(\mu). \quad (17d)$$

Note that the atmospheric transmittance in the upward direction, $T(\mu)$, has no azimuthal dependence because the diffuse Green's function depends only on the difference of azimuths $(\phi - \phi_1)$.

Thus Eq. (15) shows that, in the general case of anisotropic surface reflectance, the form of Chandrasekhar's expression for radiance is retained, given that the integral operators are substituted by the equivalent scalar functions. However, Eq. (15) cannot be used in practice. The multiple-reflection term given by the inverse operator $(\hat{I} - \hat{R}\hat{\Gamma}_{\tau_0,s}^{+})^{-1}$ can be evaluated only as the sum of series (14), $\sum_{k\geq 1} J_-^{(k)}(\tau_0)$. The number of terms in this sum required for achieving a given accuracy increases as the atmospheric opacity grows and the surface becomes more reflective. However, we show in Section 3 that we can parameterize the multiple reflections by using, at most, the first three terms of this series in calculations over land.

Returning from the operator to the integral form of notation, we can express the top-of-the-atmosphere radiance in final form as

$$I(s_0, s) = D(s_0, s) + \exp(-\tau_0/|\mu|)J(\tau_0; s) + \int_{\Omega^-} G^d(0; s_1, s)J(\tau_0, s_1)\mathrm{d}s_1, \quad \mu < 0, \quad (18)$$

where the total surface-reflected signal is represented by sum (6) or (14). Knowing the first-order radiance,

$$J^{(1)}(\tau_0; s) = S_\lambda\mu_0 \exp(-\tau_0/\mu_0)\rho(s_0, s) + \frac{1}{\pi}\int_{\Omega^+} D(\tau_0; s_0, s')\rho(s', s)\mu'\mathrm{d}s', \quad (19)$$

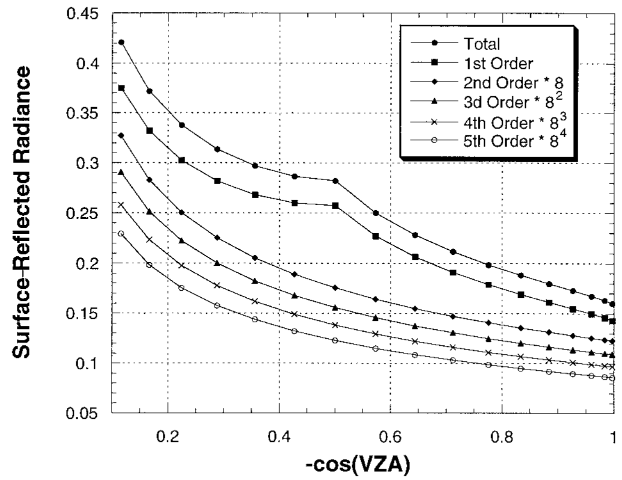

Fig. 1. Different orders of the surface-reflected radiance as functions of the view zenith angle (VZA) at $\phi = 180°$. Parameters of calculations: solar zenith angle, 60°; wavelength, 0.75 μm; aerosol optical thickness, 0.5; single-scattering albedo, 0.98; scattering function of Elterman[17] at wavelength 0.75 μm. The surface BRDF was modeled by the Rahman–Pinty–Verstraete function[18] fitted to the near-IR BRDF of grasses.[19]

we can calculate the higher orders of reflection by using Eq. (13). We can rewrite this operator formula in integral form:

$$J^{(k)}(\tau_0; s) = \frac{1}{\pi}\int_{\Omega^-} H(\tau_0; s_1, s)J^{(k-1)}(\tau_0, s_1)\mathrm{d}s_1, \quad (20)$$

where the supplementary function H is given by

$$H(\tau_0; s_1, s) = \int_{\Omega^+} G^d(\tau_0, s_1, s')\mu'\rho(s', s)\mathrm{d}s'. \quad (21)$$

The total radiance incident upon the surface is equal to

$$I(\tau_0; s_0, s) = \pi S_\lambda \exp(-\tau_0/\mu_0)\delta(s_0 - s) + D(\tau_0; s_0, s) + \int_{\Omega^-} G^d(\tau_0; s_1, s)J(\tau_0, s_1)\mathrm{d}s_1, \quad \mu > 0. \quad (22)$$

3. Practical Considerations

The derived analytical formulas, in principle, allow for the calculation of atmospheric radiance with accuracy limited only by our knowledge of the atmospheric path radiance and the Green's function. The actual accuracy of calculations depends on the order of quadrature of integration as well as on the number of multiple-reflection terms retained. By varying these parameters, we can optimize the solution for the specific applied problem in terms of speed and accuracy. In addition, we can accelerate calculations over land surfaces considerably by invoking different parameterizations of the surface-reflected radiance.

Figure 1 is an illustration of the total radiance and the first five orders of the surface-reflected radiance. The calculations were performed for grasses[19] in the near-IR range of the spectrum (0.75 μm). At a solar zenith angle of 60° and an atmospheric optical thickness of 0.5276, the albedo of grasses is 0.4806, so nearly half of the incident solar energy is reflected back into the atmosphere in each instance of reflection. The nonlinear reflection terms in Fig. 1 are scaled so as to show the close similarity in angular shape, starting from the second order of reflection. Our calculations show that, given the atmosphere–surface parameters, the ratio

$$J^{(k+1)}(\tau_0; s)/J^{(k)}(\tau_0; s) \cong \text{const} \tag{23}$$

is close to a constant independent of the illumination-view geometry. We found that relation (23) holds at $k \geq 2$ to high accuracy for common land-surface types, including vegetation, soil, sand, and snow. In the specific example described, this ratio is 0.1028 with a relative accuracy of several tenths of a percent. A similar result was independently found earlier.[20] It should be mentioned, however, that the convergence of relation (23) slows down for a ruffled water surface because of a much higher anisotropy of reflectance. In this case, as many as 4–5 orders of reflection might be needed before a constant ratio can be assumed.

A theoretical explanation of this result can be found in linear operator analysis[21] and, specifically, in its applications to the radiative transfer theory.[22,23] One of the theorems of operator analysis states that, for a continuous linear operator T defined in space of nonnegative functions u, the following relation holds, starting from some $k > 0$:

$$T^k u(s)/u(s) \cong \eta^k, \tag{24}$$

where η is a maximal eigenvalue of operator T. In our case, by substituting series (6) into lower boundary condition (4a) and by using relation (13), we can show that the lower boundary condition becomes a Fredholm equation of the second kind with the operator $T = \hat{R}\hat{\Gamma}^+_{\tau_0,s}$ and $u = J(\tau_0; s)$. Therefore we can apply relation (24) for evaluating the reflected term of the order of $k + 1$ by using its precursor as

$$J_-^{(k+1)}(\tau_0) = (\hat{R}\hat{\Gamma}^+_{\tau_0,s})J_-^{(k)}(\tau_0) \cong \eta J_-^{(k)}(\tau_0), \tag{25}$$

where η is the maximum eigenvalue of operator $\hat{R}\hat{\Gamma}^+_{\tau_0,s}$, i.e., it is a function of surface reflectance and atmospheric parameters only and does not depend on the view-illumination geometry. Therefore our above-mentioned result, relation (23), is a direct consequence of relation (24). This result also indicates that, for the problem of atmospheric radiative transfer over a land surface, relation (24) already has a convergence at $k = 2$. This result allows us to introduce an accurate parameterization:

$$J(\tau_0; s) = J^{(1)}(\tau_0; s) + \frac{J^{(2)}(\tau_0; s)}{1 - \eta}. \tag{26}$$

Equation (26) shows that the surface-reflected radiance over land can be found from the first three orders of reflection, in which the third order is used only to evaluate the parameter η numerically from relation (23). We note that the theorem in relation (24) is a powerful tool in applied mathematics that is used to accelerate convergence of iterative numerical methods.

The calculations that we performed for a variety of realistic land-cover types[24] show that, with an uncertainty of as much as a factor of 2, parameter η can be evaluated in the Lambertian approximation as $\eta \approx q(\theta_0)c_0$. This approximation becomes more accurate as the surface albedo or the anisotropy of the BRDF decreases.

Additional opportunities to accelerate computations include Lambertian forms of radiance parameterization. The most obvious one is exploited in the multiangle imaging spectroradiometer BRDF retrieval algorithm[25]:

$$J(\tau_0; s) \cong \frac{J^{(1)}(\tau_0; s)}{1 - q(\theta_0)c_0}. \tag{27}$$

We found that this approximation is accurate, to within several tenths of a percent, at the low surface reflectance typical of vegetation in the visible spectrum or at low anisotropy of the BRDF. When the surface reflectance and the anisotropy of BRDF are high, the error of relation (27) becomes nonnegligible.

Our analysis of Eq. (26) led us to a more accurate parameterization that does not have the above-mentioned limitations. To understand the derivation, let us rewrite Eq. (26) in operator form, separating the incident radiance into the direct beam $I_+^\delta = \pi S_\lambda \exp(-\tau_0/\mu_0)\delta(s - s_0)$ and path radiance:

$$\bar{I}_r{}^{\uparrow}(\tau_0; s) = \hat{R}[I_+^\delta + D_+(\tau_0)] + \frac{\hat{R}\hat{\Gamma}^+_{\tau_0}\hat{R}[I^\delta_+ + D_+(\tau_0)]}{1 - \eta}, \tag{28}$$

We can simplify the last term of Eq. (28) as follows. First, the reflected diffuse radiance $\hat{R}D_+(\tau_0)$ is already a smooth function in angles; therefore we can parameterize it by using the maximum-eigenvalue method:

$$\hat{R}\hat{\Gamma}^+_{\tau_0}\hat{R}D_+(\tau_0) \approx \eta\hat{R}D_+(\tau_0).$$

Second, we need to reduce the order of integration in the term:

$$\begin{aligned}\hat{R}\hat{\Gamma}^+_{\tau_0}\hat{R}I_+^\delta &= S_\lambda\mu_0 \exp(-\tau_0/\mu_0)\hat{R}\hat{\Gamma}^+_{\tau_0}\rho(s_0, s)\\ &= S_\lambda\mu_0 \exp(-\tau_0/\mu_0)\frac{1}{\pi}\int_{\Omega^+}\rho(s', s)\\ &\quad\times\left[\int_{\Omega^-}G^d(\tau_0; s_1, s')\rho(s_0, s_1)\mathrm{d}s_1\right]\mu'\mathrm{d}s'.\end{aligned}$$

We can do this approximately by taking the average value of the Green's function, multiplied by the cosine of the incidence angle, outside of both integral signs:

$$\hat{R}\hat{\Gamma}^{+}_{\tau_0}\hat{R}I^{\delta}_{+} \approx S_\lambda \mu_0 \exp(-\tau_0/\mu_0)\left[\frac{1}{\pi}\int_{\Omega^+}\mu' \mathrm{d}s' \int_{\Omega^-} \times G^d(\tau_0;\, s_1,\, s')\mathrm{d}s_1 \Big/ \left(\int_{\Omega^+} \mathrm{d}s' \int_{\Omega^-} \mathrm{d}s_1\right)\right] \times \int_{\Omega^+}\rho(s',\, s)\mathrm{d}s' \int_{\Omega^-}\rho(s_0,\, s_1)\mathrm{d}s_1 = S_\lambda\mu_0 \exp(-\tau_0/\mu_0)c_0{\rho_{\mathrm{av}}}^1(s){\rho_{\mathrm{av}}}^2(s_0),$$

where

$${\rho_{\mathrm{av}}}^1(s) = \int_{\Omega^+}\rho(s',\, s)\mathrm{d}s' \Big/ \int_{\Omega^+}\mathrm{d}s' = \frac{1}{2\pi}\int_{\Omega^+}\rho(s',\, s)\mathrm{d}s',$$

$${\rho_{\mathrm{av}}}^2(s_0) = \frac{1}{2\pi}\int_{\Omega^-}\rho(s_0,\, s)\mathrm{d}s. \qquad (29)$$

Evaluation of the maximum eigenvalue η in Lambertian approximation [$\eta \approx q(\theta_0)c_0$] gives the final formula for the surface-reflected radiance:

$$\bar{I}_r^{\uparrow}(\tau_0;\, s) \cong S_\lambda\mu_0 \exp(-\tau_0/\mu_0) \times \left[\rho(s_0,\, s) + \frac{c_0{\rho_{\mathrm{av}}}^1(s){\rho_{\mathrm{av}}}^2(s_0)}{1 - q(\theta_0)c_0}\right] + \frac{1}{\pi[1 - q(\theta_0)c_0]}\int_{\Omega^+} \times D(\tau_0;\, s_0,\, s')\rho(s',\, s)\mu'\mathrm{d}s'. \qquad (30)$$

The accuracy of both parametric models [relations (27) and (30)] decreases as atmospheric opacity or anisotropy of the surface BRDF increases. Therefore, to evaluate the upper bound of error, we performed the worst-case calculations for a relatively high aerosol optical thickness (0.8) for the irrigated wheat,[24] which has one of the highest anisotropies of reflectance reported in literature. Figure 2 shows the results of our calculations for these stressed conditions, presented in a form of relative errors of models (26), (27), and (30) with respect to the numerical solution by the MSH. We can see that the error of the maximum-eigenvalue method [Eq. (25)] is uniform and does not exceed ~0.5%. These results are obtained in P_{33} approximation of the MSH and for the quadrature orders in the Green's function method of 31 and 11 in zenith and azimuthal angles, respectively. By increasing these orders, we can achieve an agreement to the desired accuracy.

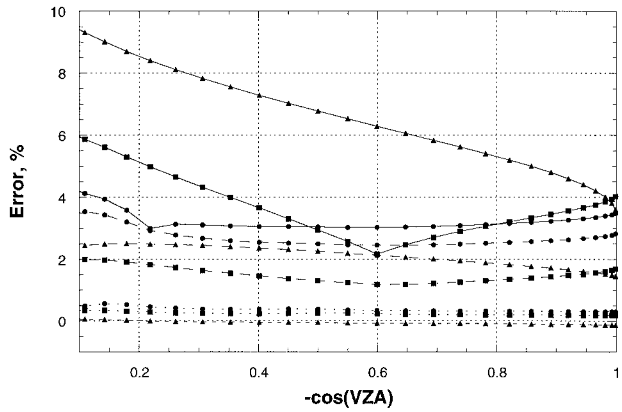

Fig. 2. Error of the total surface-reflected radiance calculated with the maximum-eigenvalue method [Eq. (26), dotted curve) and Lambertian approximations [relation (27), solid curve; relation 30, dashed curve]. Circles, squares, and triangles correspond to solar zenith angles of 77.4°, 53.2°, and 3.1°, respectively. The error is calculated with respect to the numerical MSH solution (1-I/MSH) 100%. The atmospheric parameters are the same as those of Fig. 1 except for the aerosol optical thickness ($\tau^a = 0.8$). The surface BRDF corresponds to irrigated wheat[24] in the near-IR spectral range.

The error of Lambertian approximation in relation (30) is also relatively homogeneous in zenith angle and does not exceed ~3% in the practically important range of view angles 0–78°. The typical error is considerably smaller. For the number of vegetative land covers and bare soils[24] we studied, the error is in the range from 0.1% to 0.5% in the near IR at aerosol optical thickness $\tau^a \leq 0.4$, and it is practically negligible in the visible part of the spectrum.

4. Conclusion

We have developed a rigorous analytical method for calculating atmospheric radiance with an arbitrary surface reflectance [Eqs. (6) and (18)–(22)]. The derivation for the surface-reflected radiance was based on the method of successive orders of surface interactions along with the Green's function method. The formulas obtained require knowledge of the atmospheric path radiance and the Green's function, which we can calculate rigorously by using existing numerical codes by reversing the direction of light propagation.

Our numerical study of the multiple interactions of light with surface showed that the efficiency of computations over land can be dramatically increased by use of either Lambertian or maximum-eigenvalue parameterizations. The accuracy of Lambertian parameterization [relation (30)] is generally much better than 1%; it falls below this level only in circumstances of high atmospheric turbidity over a surface of high reflectivity and anisotropy of BRDF. The maximum-eigenvalue method is distinguished by its high accuracy, which is comparable with the accuracy of rigorous numerical methods of the radiative transfer theory. To use this method, we need to calculate the first three orders of reflection, to evaluate the maximum eigenvalue at any angle by using the ratio $\eta = J^{(3)}(\tau_0; s)/J^{(2)}(\tau_0; s)$, and to calculate the land surface-reflected radiance based on Eq. (26).

References

1. J. E. Hansen and J. W. Hovenier, "The doubling method applied to multiple scattering of polarized light," J. Quant. Spectrosc. Radiat. Transfer **11,** 809–812 (1971).
2. J. V. Dave, "A direct solution of the spherical harmonics approximation to the radiative transfer equation for an arbitrary solar elevation," J. Atmos. Sci. **32,** 790–798 (1975).
3. K. Stamnes, S. C. Tsay, W. Wiscombe, and K. Jayaweera, "Numerically stable algorithm for discrete-ordinate-method radiative transfer in multiple scattering and emitting layered media," Appl. Opt. **27,** 2502–2509 (1988).
4. P. Koepke and K. T. Kriebel, "Influence of measured reflection properties of vegetated surfaces on atmospheric radiance and its polarization," Appl. Opt. **17,** 260–264 (1978).
5. E. F. Vermote, D. Tanre, J. L. Deuze, M. Herman, and J.-J. Mocrette, "Second simulation of the satellite signal in the solar spectrum, 6S: an overview," IEEE Trans. Geosci. Remote Sens. **35,** 675–686 (1997).
6. D. Tanre, M. Herman, P. Y. Deschamps, and A. de Leffe, "Atmospheric modeling for space measurement of ground reflectances, including bidirectional properties," Appl. Opt. **18,** 3587–3594 (1979).
7. A. I. Lyapustin and T. Z. Muldashev, "Generalization of Marshak boundary condition for non-Lambert reflection," J. Quant. Spectrosc. Radiat. Transfer **67,** 457–464 (2000).
8. A. I. Lyapustin, "Atmospheric and geometrical effects on land surface albedo," J. Geophys. Res. **104,** 4123–4143 (1999).
9. A. I. Lyapustin and J. L. Privette, "A new algorithm for retrieving surface BRDF from ground measurements: atmospheric sensitivity study," J. Geophys. Res. **104,** 6257–6268 (1999).
10. G. I. Bell and S. Glasstone, Nuclear Reactor Theory (Van Nostrand Reinhold, New York, 1970).
11. T. A. Sushkevich, S. A. Strelkov, and A. A. Ioltuhovskii, Method of Path Integration in the Problems of Atmospheric Optics (Nauka, Moscow, Russia, 1990).
12. S. A. W. Gerstl, "Application of the adjoint method in atmospheric radiative transfer calculations," in Atmospheric Aerosols: Their Formation, Optical Properties and Effects, A. Deepak, ed. (Spectrum, Hampton, Va., 1982), pp. 241–254.
13. S. Twomey, "Green's function formulae for the internal intensity in radiative transfer computations by matrix–vector methods," J. Quant. Spectrosc. Radiat. Transfer **33,** 575–579 (1985).
14. G. I. Marchuk and V. I. Lebedev, Numerical Methods in the Theory of Neutron Transport, (Harwood Academic, New York, 1986).
15. Y. Knyazikhin, "On the solvability of plane-parallel problems in the theory of radiation transport," USSR Comput. Math. Math. Phys. **30,** 557–569 (1990).
16. S. Chandrasekhar, Radiative Transfer (Dover, New York, 1960).
17. L. Elterman, "UV, visible and IR attenuation for altitudes to 50 km," Environ. Res. Pap-s, AFCRL, NTIS-AD 671933 (U.S. Air Force Cambridge Research Laboratories, Bedford, Mass., 1968).
18. H. Rahman, B. Pinty, and M. M. Verstraete, "Coupled surface-atmosphere reflectance (CSAR) model. 2. Semiempirical surface model usable with NOAA advanced very high resolution radiometer data," J. Geophys. Res. **98,** 20791–20801 (1993).
19. R. B. Myneni and G. Asrar, "Radiative transfer in three-dimensional atmosphere-vegetation media," J. Quant. Spectrosc. Radiat. Transfer **49,** 585–598 (1993).
20. D. J. Diner and J. V. Martonchik, "Atmospheric transfer of radiation above an inhomogeneous non-Lambertian reflective ground—II. Computational considerations and results," J. Quant. Spectrosc. Radiat. Transfer **32,** 279–304 (1984).
21. F. Riesz and B. Sz.-Nagy, Functional Analysis (Dover, New York, 1990).
22. V. S. Vladimirov, "Mathematical problems in the one-velocity theory of particle transport," Tech. Rep. AECL-1661 (Atomic Energy of Canada Ltd., Chalk River, Ontario, 1963).
23. R. K. Kaufmann, L. Zhou, Y. Knyazikhin, N. V. Shabanov, R. B. Myneni, and C. J. Tucker, "Effect of orbital drift and sensor changes on the time series of AVHRR vegetation index data," IEEE Trans. Geosci. Remote Sens. **38,** 2584–2597 (2000).
24. O. Engelsen, B. Pinty, M. M. Verstraete, and J. V. Martonchik, "Parametric bidirectional reflectance factor models: evaluation, improvements and applications," Eur. Rep. 16426 EN (Space Applications Institute, Ispra, Italy, 1996).
25. D. J. Diner, J. V. Martonchik, C. Borel, S. A. W. Gerstl, H. R. Gordon, R. Myneni, B. Pinty, and M. M. Verstraete, "MISR level 2 surface retrieval algorithm theoretical basis," NASA EOS-MISR Doc. JPL D-11401, Rev. D (NASA Jet Propulsion Laboratory, Pasadena, Calif., 1999).